Journal of Fluorescence, Vol. 8, No. 4, 1998

Further Solvatochromic, Thermochromic, and Theoretical Studies on Nile Red

Christina M. Golini,[1] Brian Wesley Williams,[1,3] and James B. Foresman[2]

Received February 25, 1998; accepted September 2, 1998

Experimental steady-state solvatochromic and thermochromic studies of Nile Red absorption and emission in nine dipolar solvents are reported, as well as theoretical modeling results concerning the ground and excited states of Nile Red in solution. Solvatochromic absorption and emission data analyzed according to conventional methods yield ground- and excited-state dipole moments of 8.9 ± 0.5 and 14.4 ± 0.5 D. Application of this conventional model to thermochromic shift data gave dipole moments of 8.4 ± 1.0 and 13.4 ± 1.0 D. The thermochromic data were also analyzed using a novel solute monopole–solvent dipole model; this model did not appear to reproduce trends in the thermochromic shift data as well as the conventional model. Results of semiempirical ZINDO/S calculations on Nile Red combined with an Onsager model for solvation were also used to examine the energetics of the excited states of Nile Red in solution. These calculations suggest the presence of a TICT state in Nile Red comparable in energy to an emitting excited state at high solvent polarity. Conventional models for solvatochromic and thermochromic response, however, appear to explain the experimental results independently of any emission from this TICT state in the present solvents.

KEY WORDS: Nile Red; solvatochromism; thermochromism; dipole moment; TICT; ZINDO/S.

INTRODUCTION

Solvatochromic molecules are of interest because of their practical utility and because describing and understanding their properties poses a continuing challenge to theory and experiment. The solvatochromic fluorophore Nile Red (Fig. 1) has been the focus of both practical and descriptive studies in recent years. For example, Nile Red has been used as a polarity probe in a variety of chemical and biophysical environments [1–4] and as the active element of a sensor capable of distinguishing different organic vapors [5]. Studies perhaps more concerned with understanding the solvatochromic response of Nile Red include those by Sarkar *et al.* [6] and Dutta *et al.* [7,8], where both the steady-state and the dynamic response of Nile Red in several different solvents and environments have been examined. The latter studies endorse the idea that a twisted intramolecular charge trans-

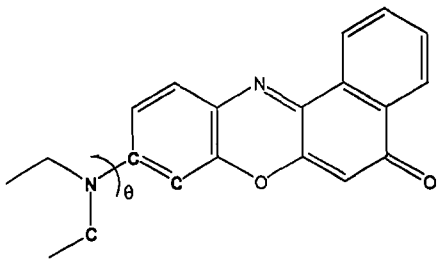

Fig. 1. Nile Red. The arrow indicates the direction in which a positive dihedral angle is defined.

[1] Department of Chemistry, Bucknell University, Lewisburg, Pennsylvania 17837.
[2] Department of Physical Sciences, York College of Pennsylvania, York, Pennsylvania 17405.
[3] To whom correspondence should be addressed.

1053-0509/98/1200-0395$15.00/0

fer (TICT) process in the excited state may play an role in understanding the solvatochromic response of Nile Red.

In the following, we wish to characterize further Nile Red through some additional experimental and theoretical studies of its properties. Experimentally, Nile Red emission in individual solvents demonstrates temperature-dependent (*thermochromic*) blue shifts with increasing temperature. Similar thermochromic effects have been observed and studied previously [9,10]; however, they do not appear to have been fully characterized for Nile Red. Investigation of thermochromic effects in Nile Red is also motivated by the appearance several years ago of an alternative description of solvatochromism and thermochromism [11]. This description attempts to explain the effects of different solvents in terms of the interaction of charged solvatochromic solute monopoles with solvent dipoles and makes quantitative predictions of the magnitude of thermochromic shifts in nonviscous solvents. Here, experimental data for Nile Red are compared to such predictions, as well as to predictions based on a simple, commonly applied model for solvatochromic fluorescent emission. With respect to theory, we also present the results of some low-level semiempirical electronic structure calculations on Nile Red. This theoretical work is motivated by the need to understand better excited-state dipole moment and energy values, especially in view of the prediction of excited-state TICT processes made in earlier studies. The present studies hence represent both an extension of and complement to the earlier work.

EXPERIMENTAL AND THEORETICAL PROCEDURES

Nile Red was obtained from either Molecular Probes (Eugene, OR) or Aldrich (Milwaukee, WI) and used without further purification. All solvents were spectral grade or better, with diethyl ether and tetrahydrofuran (THF) freshly distilled prior to solution preparation. Individual solution concentrations ranged between 2.0 and 3.5 μM throughout. Absorption spectra were collected using a Varian Cary 2300 UV–VIS–NIR spectrometer and 1-cm quartz rectangular cuvettes, with maximum solution absorbance never exceeding 0.1 absorbance unit. Fluorescence emission spectra were collected in 1-cm quartz cuvettes using a Perkin–Elmer LS-50 spectrofluorimeter equipped with a red-sensitive Hamamatsu R955 photomultiplier tube. Excitation wavelengths for each solution corresponded to the wavelength of maximum absorption, with a spectral band pass of 2.5 nm on both excitation and emission monochromators. Emission spectra collected for pure solvents revealed no fluorescent contamination. Sample technical emission spectra were corrected for instrumental response by comparison with a recrystallized *N,N*-dimethyl-3-nitroaniline standard (Aldrich), for which published emission spectra data are available between 500 and 700 nm [12]. Reported emission peaks represent weighted averages of corrected emission spectral data within 90% of the observed maxima. Sample temperatures in the emission experiments were regulated using a Neslab Endocal RTE220 constant-temperature bath connected to the cuvette holder and filled with an ethylene glycol–water mixture, with samples stirred using a magnetic stir bar. Sample temperatures were determined using a Fisher Scientific digital thermometer, with the uncertainty in solution temperature values estimated as 0.5 K. Emission spectra were generally collected for each solvent approximately every 5 K over a range spanning roughly 50 K, unless the solvent melting or boiling point fell within this range. Reported thermochromic shift values represent the slope and uncertainty of linear fits to the emission maxima data versus temperature for each solvent. The linear and nonlinear fit parameters and uncertainties reported throughout were obtained via programmable fitting function analyses of appropriate data using the general plotting and analysis program SigmaPlot 3.0 for Windows (Jandel Scientific). All theoretical calculations reported were performed using Gaussian [13] running on a Silicon Graphics R5000 Indy workstation and HyperChem 4.0 [14] running on a Intel 486 microprocessor.

EXPERIMENTAL RESULTS AND DISCUSSION

Steady-State Solvatochromism

Initially, Nile Red solvatochromism in absorption and emission was determined at room temperature in nine different aprotic solvents all possessing a dipole moment. The choice of solvents was motivated by two considerations. First, unlike some earlier studies, aprotic solvents were used exclusively in order to avoid possible hydrogen bonding interactions between the solvent and Nile Red. For alcoholic solvents, in particular, at least one earlier study of the short-term dynamics of Nile Red solvation has suggested that hydrogen bonding may affect the excited-state response [15]. Second, the alternative theory of solvatochromism cited above is applicable only to solvents having a dipole moment, so only data taken in such solvents can be compared to its

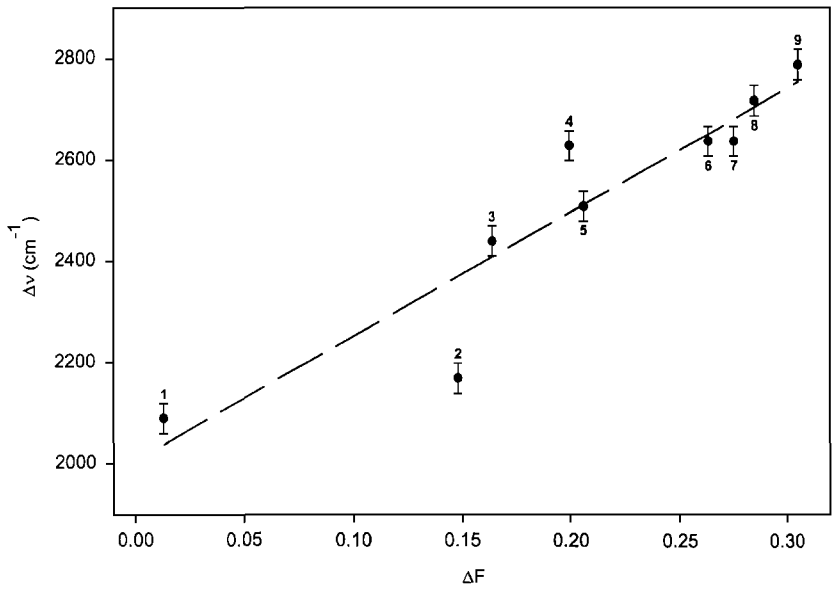

Fig. 2. Lippert plot for Nile Red. Solvents are indicated as follows: 1, toluene; 2, chloroform; 3, diethyl ether; 4, ethyl acetate; 5, tetrahydrofuran; 6, dimethyl sulfoxide; 7, dimethylformamide; 8, acetone; 9, acetonitrile

predictions. In these nine solvents, Nile Red shows increasing red shifts in both absorption and emission wavelength as solvent polarity is increased, consistent with results of earlier studies. These trends indicate that both the vertical (Franck–Condon) and the relaxed emissive excited electronic states of Nile Red possess dipole moments larger than the ground state.

From these spectral data, application of a simple model [16] approximating the solvated fluorophore as a dipole in a continuous dielectric medium permits estimation of the ground and excited-state dipole moments for Nile Red. In this model, the energy differences in absorption and emission for the fluorophore in solution compared to the gas phase are given by

$$\nu_{abs}\ (cm^{-1}) = \nu_{abs,gas} - \frac{2\mu_g\ (\mu_e - \mu_g)}{cha^3} \Delta F - \frac{2\ (\mu_e^2 - \mu_g^2)}{cha^3} f(n^2) \quad (1)$$

and

$$\nu_{em}\ (cm^{-1}) = \nu_{em,gas} - \frac{2\mu_e\ (\mu_e - \mu_g)}{cha^3} \Delta F - \frac{2\ (\mu_e^2 - \mu_g^2)}{cha^3} f(n^2) \quad (2)$$

where $\nu_{abs}(cm^{-1})$, $\nu_{em}(cm^{-1})$ are the absorption and emission energies in solution; $\nu_{abs,gas}$, $\nu_{em,gas}$ are the absorption and emission energies in the gas phase in the absence of solvent; μ_g, μ_e are the ground- and excited-state dipole moments; a is the cavity radius of the solute; c is the speed of light; h is Planck's constant; and ΔF and $f(n^2)$ are the solvent polarity functions given by

$$\Delta F = \frac{\varepsilon - 1}{2\varepsilon + 1} - \frac{n^2 - 1}{2n^2 + 1} \quad (3)$$

and

$$f(n^2) = \frac{n^2 - 1}{2n^2 + 1} \quad (4)$$

where ε equals the dielectric constant and n the refractive index of the solvent.

Upon the assumption that the gas phase energies are constant and unaffected by solvation, subtracting Eq. (2) from Eq. (1) results in the expression

$$\Delta\nu = \frac{2}{cha^3} \Delta F\ (\mu_e - \mu_g)^2 + \text{const.} \quad (5)$$

where $\Delta\nu$ is the Stokes' shift (cm^{-1}) between absorption and emission in solution. From this expression, a plot of the Stokes' shift data versus the solvent polarity parameter ΔF (deemed a Lippert plot) would be expected to be linear, with a slope proportional to the square of the difference between the ground- and the excited-state dipole moments. Figure 2 represents a Lippert plot of the Stokes' shifts observed for Nile Red in the nine solvents

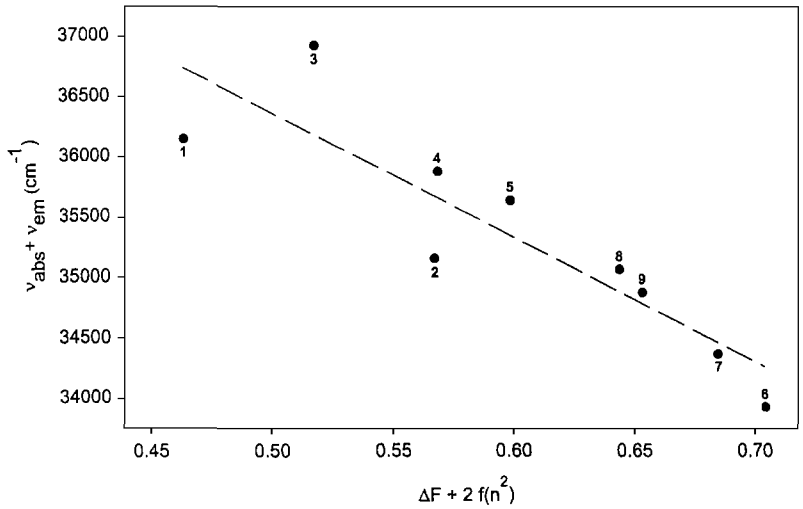

Fig. 3. Equation (6) for experimental absorption and emission energies. Solvents are labeled as in Fig. 2. Here, the slope of the linear fit is proportional to the value $\mu_e^2 - \mu_g^2$, where μ_g and μ_e are the ground and excited state dipole moments.

indicated. From the slope of a linear fit to these data (2460 ± 370 cm^{-1}), the conversion 1 $Debye^2/Å^3 = 5035$ cm^{-1}, and the assumption of a cavity radius a of 5 Å, a dipole moment difference ($\mu_e - \mu_g$) of 5.5 ± 0.5 D is obtained. This value is roughly 1 Debye lower than values obtained from similar plots in earlier reports [7 and references cited], although it still represents a considerable increase in the dipole moment for Nile Red upon excitation. The basis for the difference in values observed between this and earlier studies appears to lie mainly in the choice of solvents; earlier studies, for example, included Stokes' shifts obtained in nonpolar solvents such as cyclohexane as well as in alcoholic solvents. This large dipole moment difference, as well as the solvent polarity dependence of the fluorescence quantum yield observed in earlier studies, leads to the suggestion that a polarity-dependent TICT process in the excited state may influence the observed solvatochromic response.

The same experimental absorption and emission data used to estimate the dipole moment difference between the ground and the excited state can also be used to estimate the difference in the squares of the ground and the excited-state dipole moments. Addition of Eqs. (1) and (2) results in the expression

$$\nu_{abs} + \nu_{em} = \frac{-2\,(\mu_e^2 - \mu_g^2)}{cha^3} \left(\Delta F + 2\, f(n^2)\right) + \text{const.} \tag{6}$$

such that the sum of the absorption and emission energies in solution plotted against the function [$\Delta F + 2\, f(n^2)$] would be expected to be linear with a slope proportional to the difference in the squares of the dipole moments. Figure 3 represents a plot of the experimental data corresponding to Eq. (6). From the slope (− 10,360 ± 2050 cm^{-1}) of a linear fit to this plot and the assumption of a 5-Å cavity radius made previously, a value of 128.6 ± 25.4 D^2 results for the difference in the square of the dipole moment values. Comparing this to the dipole moment difference 5.5 ± 0.5 D from Fig. 2 leads to estimates of 8.9 ± 0.5 and 14.4 ± 0.5 D for the ground- and excited-state dipole moments of Nile Red from the steady-state solvatochromic data.

Thermochromism

Besides showing polarity dependent shifts in absorption and emission, Nile Red in solution also demonstrates blue shifts in emission in individual fluid solvents as the temperature is increased. As an example, Fig. 4 shows how observed emission peak energies for Nile Red in acetone vary as a function of temperature. Over this temperature range, the emission peak energy appears to increase linearly as the temperature is increased. Table I lists thermochromic shift values (cm^{-1}/K) derived from linear fits to data similar to that shown in Fig. 4 for each of the nine solvents reported in Figs. 2 and 3. Such thermochromic shift data is of interest for at least two reasons: first, it can serve as an experimental test of different theories or models of solvation, and second,

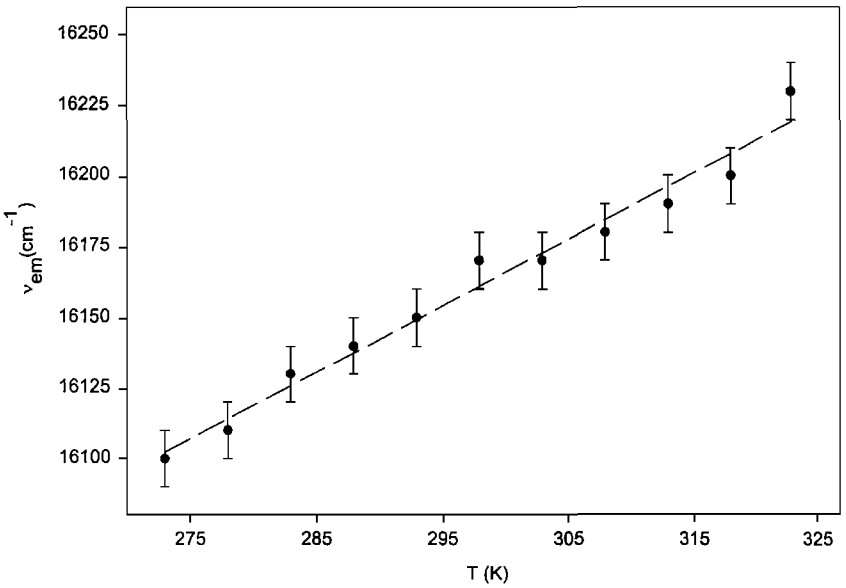

Fig. 4. Thermochromic emission shifts for Nile Red in acetone. Emission peak energies for Nile Red in acetone increase with increasing temperature near room temperature. Similar thermochromic shifts were observed and measured for the other eight solvents. The thermochromic shift in acetone was taken from the linear fit to be 2.4 ± 0.1 (cm^{-1}/K).

under the assumption of a particular theory or model, it can serve as a method for estimating ground and excited state dipole moment values.

Taking the temperature derivative of Eq. (2) should give the corresponding expression for the expected emission thermochromic shift in an individual solvent for this model. Under the simplifying assumption that only the solvent polarity functions vary with temperature, the expression

$$\frac{d}{dT}\nu_{em} = -\frac{2\mu_e(\mu_e - \mu_g)}{cha^3}\frac{d}{dT}\Delta F - \frac{2(\mu_e^2 - \mu_g^2)}{cha^3}\frac{d}{dT}f(n^2) \quad (7)$$

results. Table III shows the results of a non-linear fit of Eq. (7) to the experimental thermochromic shift data obtained for the nine solvents shown in Table I. The ground- and excited-state dipole moment values were treated as fitting parameters in the nonlinear fit, with their difference constrained to lie between 5.0 and 7.0 D on the basis of the uncertainty in the earlier Lippert plot analysis. As previously, a cavity radius of 5 Å was assumed. The dielectric constant and refractive index values and temperature derivatives used for each solvent in these fits are given in Table I. These values were derived from linear fits to published data for the dielectric constant and refractive index for each solvent over the temperature range of interest; they represent the fitted values at 298 K.

The ground- and excited-state dipole moment values for the fit shown in Table III using Eq. (7) were 8.4 ± 1.0 and 13.4 ± 1.0 D, respectively. These values generally reproduce the thermochromic shift data and give reasonable, if not exact, magnitudes for the expected thermochromic shift values for each individual solvent. This equation appears to have the greatest degree of difficulty in fitting the experimental data for the moderate polarity solvents diethyl ether and ethyl acetate, as well as the dipolar aromatic solvent toluene. For diethyl ether, a distinguishing factor may be that at 298 K, the solvent for this solution lies only 10 K below its boiling point, which might affect solvent–solute interactions. For toluene, it may be that a specific, rather than general, solvent–solute interaction occurs as has been suggested for benzene [17]. However, the discrepancy with ethyl acetate is somewhat harder to rationalize, particularly in that this solvent is generally considered to be "well behaved" in most solvatochromic studies. The errors reported for the dipole moment values were determined using the "jackknife" statistical procedure [18]. Combining these values with the estimates obtained from steady-state spectral data gives overall experimental estimates for the ground- and excited-state

Table I. Solvent Parameters and Thermochromic Shift Values for Nile Red in Several Solvents[a]

Solvent	ε	$-(d\varepsilon/dT)$	n	$-(dn/dT)$	Thermochromic shift (cm^{-1}/K)
Toluene	2.37	0.0023	1.4938	0.00056	3.3 ± 0.2
Diethyl ether	4.23	0.025	1.35031	0.00055	3.6 ± 0.5
Chloroform	4.78	0.021	1.4431	0.00053	4.0 ± 0.2
Ethyl acetate	6.00	0.016	1.3702	0.00045	3.2 ± 0.2
Tetrahydrofuran	7.22	0.034	1.4036	0.00049	2.5 ± 0.2
Acetone	20.80	0.100	1.3563	0.00052	2.4 ± 0.1
Dimethylformamide	37.10	0.210	1.4275	0.00061	1.6 ± 0.1
Acetonitrile	37.1	0.200	1.3421	0.00045	1.2 ± 0.2
Dimethyl sulfoxide	46.50	0.130	1.476	0.00041	0.9 ± 0.1

[a]Reported thermochromic shift values are taken from linear fits to corrected emission spectra for each solvent taken over several temperatures (e.g., Fig. 4). These parameters were used in fitting Eq. (7) to the experimental thermochromic shift data (Table III).

Table II. Solvent Parameters for Eq. (9)[a]

Solvent	d (Å)	μ (D)	γ (K^{-1})
Toluene	4.1	0.31	0.001067
Diethyl ether	3.5	1.15	0.000126
Chloroform	3.7	1.15	0.001654
Diethyl ether	3.5	1.15	0.000126
Ethyl acetate	3.4	1.82	0.00139
Tetrahydrofuran	3.6	1.75	0.00138
Acetone	3.5	2.69	0.00143
Dimethylformamide	3.6	3.24	0.001
Acetonitrile	3.5	3.53	0.001368
Dimethyl sulfoxide	4.1	4.06	0.0000928

[a]The parameters given below were used in fitting Eq. (8) to the thermochromic data, with the results shown in Table III. Symbols are as defined in the text, with values for μ and γ taken from Riddick *et al.*, *Organic Solvents* (4th ed.), Wiley, New York, 1986.

Table III. Experimental and Calculated Thermochromic Shift Values for Nile Red in Several Solvents[a]

Solvent	Exp. shift	Eq. (7) cm^{-1}/K	Eq. (8)
Toluene	3.3 ± 0.2	1.7	0.2
Diethyl ether	3.6 ± 0.5	5.2	1.7
Chloroform	4.0 ± 0.2	3.6	1.4
Ethyl acetate	3.2 ± 0.2	2.1	2.1
Tetrahydrofuran	2.5 ± 0.2	2.9	1.9
Acetone	2.4 ± 0.1	1.5	2.7
Dimethylformamide	1.6 ± 0.1	1.3	2.2
Acetonitrile	1.2 ± 0.2	1.2	3.2
Dimethyl sulfoxide	0.9 ± 0.1	0.7	2.3

[a]Thermochromic shift values for Nile Red emission were calculated through nonlinear fits of Eqs. (7) and (8) using the parameters in Tables I and II (see text). The ground- and excited-state dipoles for Nile Red used in Eq. (7) were 8.4 ± 1.0 and 13.4 ± 1.0 D; for Eq. (8) the ground-state dipole was 7.2 ± 3.6 D, with the excited-state dipole taken to be 2.1 ± 0.3 of this value.

dipole moment values for Nile Red in solution of about 8.6 and 14.0 D, respectively.

An alternative theory of thermochromic shifts in emission was derived some time ago by Macgregor and Weber [11]. Rather than working on the basis of continuum models of solvation, their model represents solute dipole solvation in terms of distributions of solvent dipoles about solute monopoles. These authors suggest that the expression

$$\frac{d}{dT}\nu_{em} = \frac{k}{hc}(m-1)\left[1 - \alpha^2\,\mathrm{csch}^2\,\alpha + (2/3)\,\gamma\,T(\alpha\,\mathrm{ctanh}\,\alpha - \alpha^2\,\mathrm{csch}^2\,\alpha)\right] \tag{8}$$

generally accounts for thermochromic shifts of polar solute emission in dipolar solvents. In Eq. (8), k is the Boltzman constant, m is the ratio of the excited state and ground state dipole moments, T is the temperature (K), γ is the thermal expansion coefficient of the solvent, and α is a reduced parameter defined by

$$\alpha = \frac{m\,\mu\mu_g}{d^2\,lk} \tag{9}$$

where μ is the solvent dipole moment, d is a distance defined as the sum of the Van der Waals radii of the atoms supporting the solute monopoles and the oppositely charged end of the solvent dipole, plus the interatomic distance of the dipole ends in the solvent molecule, and l is the distance between the solute dipole moment monopoles. Here, l was taken to be 9.4 Å.

Table III also gives a best fit of Eq. (8) to the experimental thermochromic data using the parameters shown in Table II. The values of m and μ_g were treated as fitted parameters in our analysis, corresponding to 2.1 ± 0.3 and 7.2 ± 3.6 D, respectively. Again, the errors

were estimated using the "jackknife" statistical procedure [18]. Determination of appropriate values for d in Eq. (9) is problematical in that for many of the solvents, the dipole moment is not clearly defined as lying between just two atoms, and because d also depends to some extent on the relative orientation of solvent and solute at the two different monopoles of the solute. The values in Table II hence represent what we consider to be reasonable estimates based on the presumed positions of the dipole moment in each solvent molecule and how they can orient with respect to the solute monopoles. Even given this limitation in the determination of d, the fit shown in Table III suggests that without fairly large adjustments in the parameter values used, this alternative picture of solvation does not appear to account for the observed thermochromic data as well as the simple continuum model of solvation given above.

While the simple model of thermochromism presented above appears to represent better the observed trends in different dipolar solvents than the alternative monopole model, it also has difficulties in exactly reproducing observed values for several solvents. Continuing exploration of thermochromic phenomena for other solvatochromic fluorophores, as well as the application of more sophisticated models such as that of Rolinski and Balter [19] appears warranted.

THEORETICAL RESULTS AND DISCUSSION

Besides experimental investigation of its solvatochromism and thermochromism in several solvents, semiempirical electronic structure calculations using the ZINDO/S model were also performed for Nile Red. This semiempirical method has been specifically parameterized to reproduce experimental absorption spectra. The primary purpose of these calculations was assess whether or not a TICT state might be present in Nile Red, and if present, how it might affect interpretation of the current experimental results. Computationally, the calculation of excited-state properties as well as the effects of solvation for a molecule the size of Nile Red presently represents a considerable challenge for theory; the development of methodologies dealing with both factors is the subject of active research. Consequently, the results reported below really represent only a first attempt to model ground and excited state Nile Red properties in solution with several simplifying assumptions. Initially, the basic Nile Red geometry was taken to be that found for the ground state in the gas phase from minimization at the RHF/3-21G ab initio level; in further ZINDO/S calculations, all bond lengths and angles except for the CNCC dihedral (see Fig. 1) were held fixed at these values. The diethyl amino substituent on Nile Red essentially defines a single plane connected to a second plane defined by the remainder of the molecule. The excited-state properties reported hence correspond to geometries representing vertical excitation from ground states where only the CNCC dihedral angle (that is, the relative orientation of the two planes) was varied for each geometry. The ZINDO/S calculations use a configuration interaction among all singly substituted determinants to represent the excited state. The configuration space was determined by truncating the determinants whose energy was greater than 12.00 eV above the ground state.

The energetic effect of solvation at these ground- and excited-state geometries was determined from an Onsager reaction field model, where the solute is represented as a dipole contained in a spherical cavity of radius a in a continuous solvent medium of dielectric constant ε. This results in an energy stabilization between the gas phase and the solution for a solute with dipole moment μ of

$$\Delta E = \frac{2(\varepsilon - 1)\,\mu^2}{(2\varepsilon + 1)\,a^3} \tag{10}$$

As in the experimental analysis above, a cavity radius of 5 Å was also assumed, where the dipole moment of the ground and excited states represent gas phase values at the specified dihedral angles.

Figure 5 and Table IV summarize the results of gas phase ZINDO/S calculations for the ground and first five singlet excited states of Nile Red at several different CNCC dihedral angles with the assumptions noted. In the gas phase, the ground and excited states all appear to show energetic minima at dihedral angles of roughly 30°. The ground-state dipole moment value, ~ 6 D, is somewhat lower than the estimate of ~ 8.6 D obtained from the solution spectral data. The results indicate the first two excited states are nearly degenerate in energy at their minima, but differ greatly in their dipole moment values, with state 2 having a dipole moment roughly 13–14 D greater than state 1. The higher energy states 3 and 4 also show increases in dipole moment compared to the ground state and state 1, although not as large as state 2. As the dihedral angle is increased to 90° and beyond, states 1, 3, and 4 maintain roughly similar energy differences; state 2 increases relative to state 1 as the angle is increased, while state 5 shows a slight decrease in energy upon approaching 90°. For state 5, the energy change is accompanied by a large increase in the dipole moment to roughly 21 D.

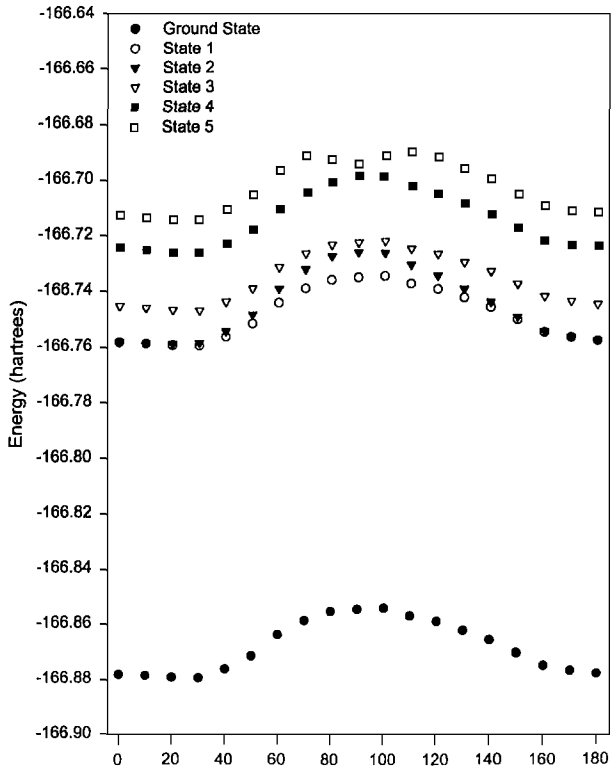

Fig. 5. ZINDO/S energy calculations for the ground and first five excited states of Nile Red. Energies were calculated starting with a fixed RHF/3-21G ab initio geometry where the CNCC dihedral angle was then varied. Dipole moment values associated with each point are shown in Table IV.

Table IV. Calculated Dipole Moments for the Ground and First Five Excited States of Nile Red[a]

Dihedral angle (deg)	Ground state	State 1	State 2	State 3	State 4	State 5
0	6.23	9.72	6.67	10.74	10.04	4.72
10	6.20	5.89	10.45	10.70	9.89	4.61
20	6.12	1.89	14.89	10.63	10.00	4.48
30	5.99	1.58	15.83	10.52	10.05	4.47
40	5.81	1.71	15.77	10.37	10.09	4.45
50	5.61	1.87	15.31	10.18	10.12	4.45
60	5.41	2.01	14.55	10.00	10.17	4.58
70	5.25	2.14	13.58	9.85	10.13	7.71
80	5.15	2.22	12.64	9.75	9.92	18.04
90	5.11	2.25	12.44	9.72	7.56	21.92
100	5.15	2.22	12.73	9.76	9.40	18.49
110	5.27	2.13	13.71	9.85	9.78	7.71
120	5.43	2.03	14.69	9.99	9.97	4.61
130	5.62	1.92	15.47	10.16	10.03	4.44
140	5.81	1.83	16.03	10.34	10.06	4.42
150	5.99	1.78	16.39	10.50	10.09	4.45
160	6.13	1.81	16.67	10.64	10.12	4.48
170	6.22	1.77	16.67	10.73	10.09	4.62
180	6.23	9.72	6.67	10.74	10.04	4.72

[a]Entries represent the dipole moments determined from ZINDO/S calculations for each state at the CNCC dihedral angle indicated. Except for the dihedral angle, molecular geometries are fixed at the RHF/3-21G *ab initio* geometry determined for Nile Red. Values are Debyes.

Application of the Onsager reaction field model at dielectric values of 2.0, 8.0, 20.0, and 80.0 to the data in Table IV indicates that at all dielectric values, state 2 has the lowest energy minima of all five states, while state 5 has the next lowest minima at the highest three values of the dielectric constant. Figure 6 shows how the relative energies of states 2 and 5 vary for different dihedral angles and increasing dielectic constant. The experimentally observed red shifts in absorption wavelength with increasing polarity are consistent with an increase in dipole moment upon vertical excitation from the ground state. Hence, in these calculations, state 2 would appear best to represent the lowest energy vertical excited state for Nile Red in solution, while state 5 would appear to represent a TICT excited state. Due to the larger dipole moment associated with state 5, the energy difference between these two states decreases with increasing dielectric constant, although the state 5 energy minima always remains above the state 2 minima. The energy difference between the minima amounts to ~4400 cm^{-1} at the highest dielectric constant values from the calculations.

These results may not truly model Nile Red in solution due to the simplifying assumptions made. The potential energy surfaces (PES) calculated here show states whose energies cross. Configuration interaction from singles cannot fully treat this situation (a multideterminantal wavefunction is needed such as is available in the CASSCF [20] model). However, the qualitative information suggested by the simple modeling presented is useful. While the calculations indicate a difference between the ground-state and the excited-state dipole moments somewhat larger than the experimental value (~9 vs 5.5–7.0 D), they also indicate a dipole moment value for an excited state in solution (~15 D) comparable to that obtained from experiment (~14 D). They also suggest the existence of a TICT state roughly comparable in energy to this excited state at high solution polarity. These energy calculations cannot indicate whether or not this TICT state is emissive. However, earlier experimental observations indicate decreases in fluorescence yield and lifetime with increasing solvent polarity. Additionally, the calculated dipole moment for the TICT state (~21 D) is significantly larger than that determined from the solvatochromic and thermochromic data. Considering the experimental and theoretical results together, it would appear that there is no need to invoke TICT state

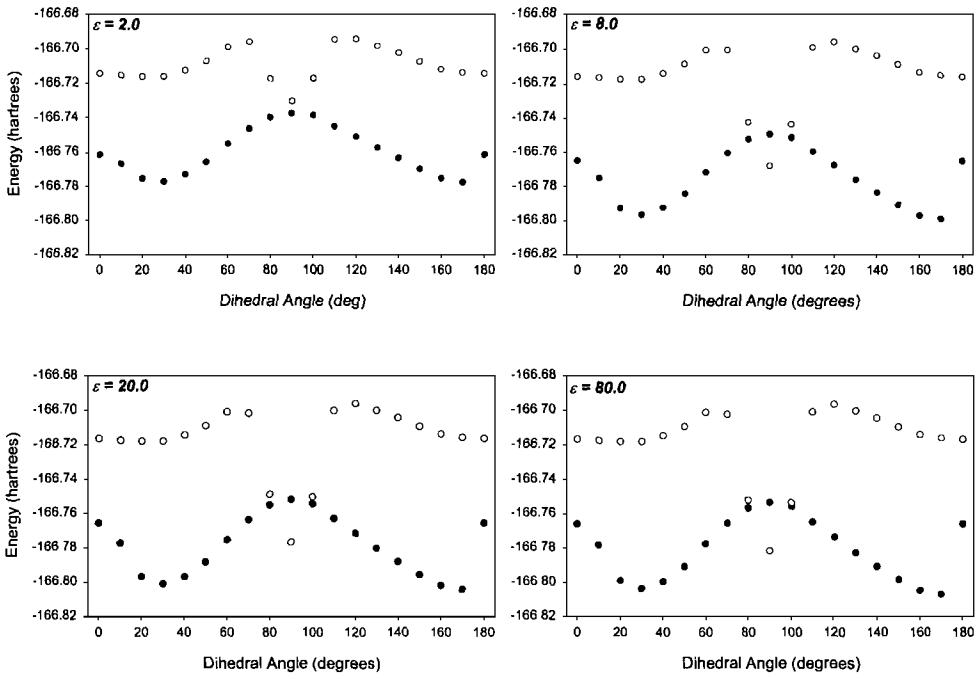

Fig. 6. Relative energies of excited states 2 and 5 as a function of CCNC dihedral angle and dielectric constant. The relative energies of states 2 and 5 are shown as a function of dihedral angle at various bulk solution dielectric constants ε, using Eq. (10). As the solution polarity increases, the energy of state 5 at a dihedral angle of 90° approaches that of state 2 at 30°. State 2, filled circles; state 5, open circles.

emission in order to explain the experimental solvatochromic and thermochromic observations in the present set of solvents.

CONCLUSIONS

Several conclusions can be reached from the present results on Nile Red. The steady-state spectral data analyzed according to a simple model are consistent with earlier studies indicating a substantial increase in the dipole moment of Nile Red upon excitation, although perhaps not as large a change as reported earlier. Analysis of thermochromic data indicates that the same simple model appears to represent reasonably, although not exactly, trends in Nile Red emission behavior in different solvents as solution temperatures are changed near room temperature. This simple description also appears to be better than a previously proposed model based on solute monopole–solvent dipole interactions. Finally, ZINDO/S semiempirical calculations on Nile Red performed with simplifying assumptions as to excited-state geometry and the energetic effects of solvation suggest the presence of a TICT state. According to the calculations, this TICT state is roughly comparable in energy to the lowest-energy excited state at high solvent polarities, and has a dipole moment significantly higher than the emitting excited state. These calculations hence support suggestions made in earlier studies of the existence of such a TICT state. However, the experimental spectral data in the present set of solvents appear to be explained adequately without any possible emission from this TICT state.

ACKNOWLEDGMENTS

B.W.W. would like to acknowledge the Donors of the Petroleum Research Fund, administered by the American Chemical Society, for support of this research. J.B.F. would like to thank Gaussian, Inc., for their financial support of this work.

REFERENCES

1. S. B. Ruvinov, X. -J. Yang, K. D. Parris, U. Banik, S. A. Ahmed, E. W. Miles, and D. L. Sackett (1995) *J. Biol. Chem.* **270**, 6357–6369.
2. D. L. Sackett, J. L. Knutson, and J. Wolff (1990) *J. Biol. Chem.* **265**, 14899–14906.

3. K. Goodling, K. Johnson, L. Lefkowitz, and B. W. Williams (1994) *J. Chem. Ed.* **71**, A8–A12.
4. D. M. Davis, and D. J. S. Birch (1996) *J. Fluoresc.* **6**, 23–32.
5. T. A. Dickinson, J. White, J. Kauer, and D. R. Walt (1996) *Nature* **382**, 697–700.
6. N. Sakar, K. Das, D. N. Nath, and K. Bhattacharyya (1994) *Langmuir* **10**, 326–329.
7. A. K. Dutta, K. Kamada, and K. Ohta (1996) *J. Photochem. Photobio. A* **93**, 57–64.
8. A. K. Dutta, K. Kamada, and K. Ohta (1996) *Chem. Phys. Lett.* **258**, 369–375.
9. A. Bauman (1989) in B. W. Rossiter and J. F. Hamilton (Eds.), *Physical Methods of Chemistry 3B*, 2nd. ed., John Wiley and Sons, New York.
10. A. Kawski (1990) in J. F. Rabek (Ed.), *Progress in Photochemistry and Photophysics* **5**, CRC Press, Boca Raton, FL., pp. 1–47.
11. R. B. Macgregor and G. Weber (1981) *Ann. N.Y. Acad. Sci.* **366**, 140–154.
12. A. Schmillen and R. Legler (1967) *Landolt-Bornstein-Numerical Data and Functional Relationships in Science and Technology*. Group II: Atomic and Molecular Physics, Vol. 3. Luminescence of Organic Substances (K. H. Hellwege, Ed.), Springer-Verlag, New York, p. 228.
13. M. J. Frisch, G. W. Trucks, H. B. Schlegel, P. M. W. Gill, B. G. Johnson, M. A. Robb, J. R. Cheeseman, T. Keith, G. A. Petersson, J. A. Montgomery, K. Raghavachari, M. A. Al-Laham, V. G. Zakrezewski, J. V. Ortiz, J. B. Foresman, J. Cioslowski, B. B. Stefanov, A. Nanayakkra, M. Challacombe, C. Y. Peng, P. Y. Ayala, W. Chen, M. W. Wong, J. L. Andres, E. S. Reploge, R. Gomperts, R. L. Martin, D. J. Fox, J. S. Brinkley, D. J. Defrees, J. Baker, J. P. Stewart, M. Head-Gordon, C. Gonzalez, and J. A. Pople, *Gaussian 94*, Revision D.3, Gaussian, Inc., Pittsburgh PA (1995).
14. Hyperchem 4.0 (1994) HyperCube, Inc., 1115 NW 4th Street, Gainesville, FL 32601.
15. B. A. Bushuk, A. N. Rubinov, and A. P. Stupak (1991) *Exp. Tech. Phys.* **39**, 347–350.
16. J. R. Lakowicz (1983) *Principles of Fluorescence Spectroscopy*, Plenum, New York, Chap. 7.
17. B. Koutek (1978) *Coll. Czech. Chem. Comm.* **43**, 2368–2386.
18. M. S. Caceci (1989) *Anal. Chem.* **61**, 2324.
19. O. Rolinski and A. Balter (1995) *J. Fluoresc.* **5**, 321–328.
20. M. P. Fulscher, K. Andersson, and B. O. Roos. (1992) *J. Phys. Chem.* **96**, 9204–9212.